ISSN: 0067-2904

# Solvothermal Synthesis and Characterization of Indium Oxid Nanoparticles

**Rashed T. Rasheed[1], Saryia D. Al-Algawi[2], Layla A. Jaffer[2*]**

[1] Applied Chemistry Division, School of Applied Sciences, University of Technology, Baghdad, Iraq.
[2]Applied Physics Division, School of Applied Sciences, University of Technology, Baghdad, Iraq.

**Abstract**

In this study, $In_2O_3$ was prepared by Solvothermal technique in autoclave device, which is a simple and inexpensive technique to indicate the best condition. The reaction took place between indium chloride and urea. $In(OH)_3$ as-prepared annealing at 100°C and convert to $In_2O_3$ at annealing temperatures 300, 500, 700 °C for 90 min .The physical properties of nanoparticles were characterized by XRD, SEM, AFM, UV/Visible and FTIR spectroscopy measurements. The examination results of XRD for $In_2O_3$ powder annealed at different temperature showed the formation of a cubic phase of nanoparticles with high intensity of plane (222). The lattice constant decreases with the increase of annealing temperature (from 10.07 to 10.04 Å). AFM indicated an increase in grain size of $In_2O_3$ with increasing of annealing temperatures (from 78.59 to 94.4 nm). The optical properties, transmittance of $In_2O_3$ nanoparticles at annealing temperatures 500°C have a high transparent reach to (89%) and Energy gap Increases with increasing annealing temperature in range (3.6 to 4.65 eV).

**Keywords:** Indium oxide **($In_2O_3$)**, Solvothermal, cubic structure, transmittance.

# دراسة الخصائص لأوكسيد الأنديوم النانوية

**راشد طالب رشيد[1]، سارية ذياب العلكاوي[2]، ليلى علي جعفر[2*]**

[1]فرع الكيمياء التطبيقية، قسم العلوم التطبيقيه، الجامعة التكنلوجية، بغداد، العراق

[2] فرع الفيزياء التطبيقية، قسم العلوم التطبيقيه، الجامعة التكنلوجية، بغداد، العراق

**الخلاصة**

في هذا البحث، تم تحضير اوكسيد الانديوم بتقنية الضغط الحراري باستخدام جهاز الأوتكليف ، وهي تقنية سهلة ورخيصة للحصول على افضل تفاعل بين كلوريد الانديوم و اليوريا. تم تحويل هايدروكسيد الانديوم الملدن بدرجة حراره 100م° الى اوكسيد الانديوم عند درجات الحراره 300، 500، 700م° لفتره 90 دقيقة. شخصت الخواص الفيزيائية للجسيمات النانوية بواسطة قياسات حيود الأشعة السينيه ، المجهر الألكتروني الماسح مجهر القوة الذرية، الأشعة فوق البنفسجية/المرئية و مطيافية الأشعة تحت الحمراء. اظهرت نتائج فحص حيود الأشعة السينية للجسيمات الملدنة عند الدرجات الحرارية المختلفة الى تكون الطور المكعبي للتركيب البلوري لأوكسيد الأنديوم مع ظهور شدة عالية للقمة (222) وتبين ان ثابت الشبيكة يقل بزيادة درجة حرارة التلدين (من 10.07الى 10.04 انكستروم). بينت نتائج فحوصات مجهرالقوة الذرية هناك زيادة في

*Email: Laglaali89m@yahoo.com

الحجم الحبيبي لاوكسيد الانديوم (من78.59 الى 94.4 نانومتر) مع زيادة درجة حرارة التلدين.اضهرت الخصائص البصرية ان اوكسيد الانديوم النانوي انة يمتلك نفاذية عالية تصل الى (89%) عند درجة تلدين (500 م°) و زيادة فجوات الطاقة مع زيادة درجات حرارة التلدين لتتراوح (3.6−4.65 الكترون فولت).

## 1. Introduction

Indium oxide ($In_2O_3$) is among the important transparent conducting materials (TCO), Indium oxide ($In_2O_3$) is an n-type semiconductor which has high transparency (>70%) to visible light [1] and wide band gaps of (3-4.5 eV) [2]. The structure of $In_2O_3$ in its crystalline form is body centered cubic with lattice constant a = 10.118 Å. It can be prepared by a variety of techniques such as chemical vapor deposition [3], pulsed laser deposition [4], sol–gel [5] and hydro-thermal [6, 7]. The application of nanoparticle of $In_2O_3$was found in many technological applications in electronic devices of various types like: transparent windows in liquid crystal displays, anti-refraction coatings, electro chromic devices [3], liquid crystal displays [8] , gas sensors, solar cells and photovoltaic devices [9,10]. The gas-sensing materials have been used for detecting various gasses, such as ammonia, ethanol, hydrogen, methane, butane and carbon monoxide [7, 11].

The crystalline structure, morphology and particle size of the $In_2O_3$ were investigated using XRD, SEM, AFM, UV–visible and FTIR spectroscopy measurements and electrical properties for $In_2O_3$ nanostructures.

## 2. Experimental part

Indium oxide nanoparticles were synthesized by Solvothermal technique using autoclave, by reaction of indium chloride with urea. Indium chloride ($InCl_3$) (3 g) dissolved in distilled water. The solution was stirred with a magnetic stirrer at 25 °C for 10 min in a beaker until it became colorless. Meanwhile, in another beaker, urea ($NH_2CONH_2$), (1.2260 g) dissolved in distilled water. The solution was stirred with a magnetic stirrer at 25 °C for 10 min in a beaker until it became colorless. The two solutions were mixed and stirred with a magnetic stirrer at 25 °C for 20 min until it became colorless, after that the mixed solutions were added into a 50 ml Teflon-lined autoclave. The autoclave was sealed and put into an oven at 200 °C for 5 h. Then, the autoclave was allowed to cool to room temperature naturally. The white precipitate ($In(OH)_3$) was washed with distilled water (about 5 times), and collected by centrifugation, washed with ethanol (2 times) and annealing at the different temperature (100,300,500,700 °C) for 90 min, After annealing at (300, 500, 700 °C), the powder convert to yellow color ($In_2O_3$), this shown in Figure-2.

The reaction took place between the indium chloride and urea to product white precipitate according to the general reaction equations as following steps:

1. $3NH_2CONH_2+9H_2O \longrightarrow 6NH_4OH+3CO_2$ …… … (1)
2. $2InCl_3+6\ NH_4OH \longrightarrow 2In\ (OH)_3+6NH_4Cl$ …… … … (2)
3. $2In\ (OH)_3 \xrightarrow{Heat} In_2O_3 + 3H_2O$ …… … (3)

The final equation is:

$$2InCl_3 + 3NH_2CONH_2 + 6H_2O \xrightarrow{Heat} 2InO_3 + 6NH_4Cl + 3CO_2 \quad \ldots\ldots\ldots\ldots \quad \ldots(4)$$

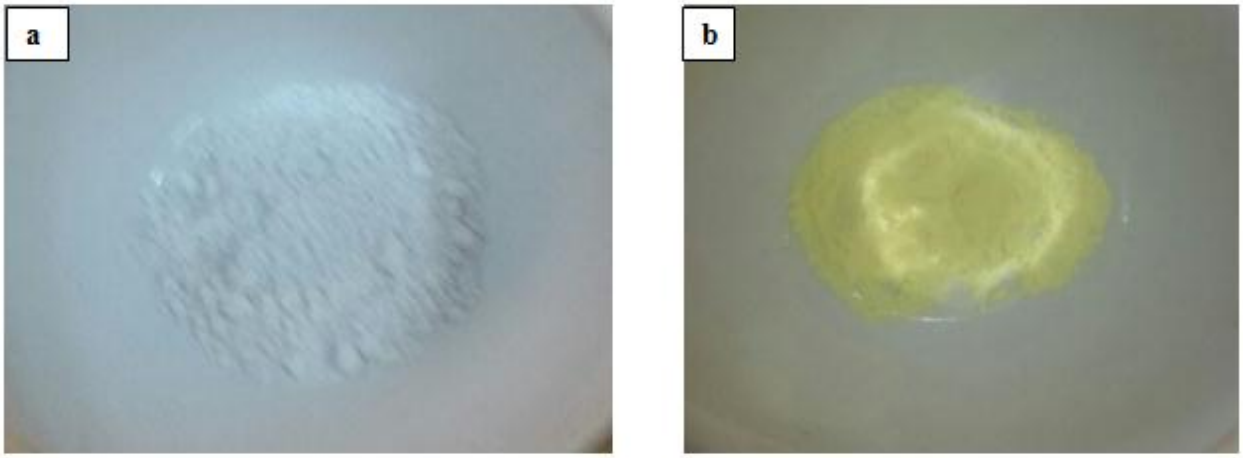


**Figure 1- a) indium hydroxide at 100°C, b) indium oxide at 300°C**

## 3. Results and Discussion

Figure -2 show XRD for indium oxide $In_2O_3$. The annealing temperature is the important effect on the structure of indium oxide nanoparticles. The XRD pattern can be well indexed the phase structure of the $In(OH)_3$ and its thermally manufactured products ($In_2O_3$) at (100°C), Figure-2(a) shows four diffraction peaks (200),(220),(420) and (422) at (2θ=22.4276, 31.8188, 51.2987 and 56.6070°), All XRD patterns correspond well to the bcc structure of indium hydroxide $In(HO)_3$ according to the (JCPDS Card No.16-0161). The annealing at (300°C) convert $In(OH)_3$ to $In_2O_3$ so another different peaks appears (200),(222), (440) and (400) at(2θ=21.6260,30.7057, 51.1266 and 35.5837°) this shows in Figure-2(b). The annealing at (500°C) Figure-2(c) shows different peaks (200), (222), (440) and (400) at (2θ=21.6681, 30.7517, 51.1982 and 35.6324°). The annealing at (700°C) Figure-2(d) shows different peaks (200), (222), (440) and (400) at (2θ=21.7106, 30.8050, 51.2514 and 35.6800°), respectively that are close to the values of the reference data ( JCPDS Card No: 44-1087.). The intensity ratio of the peaks (200), (440) and (400) decreases and increases in (222) orientation when the annealing temperature was increased. The crystallite size and the energy of the surface species increases with increasing annealing temperature [3].

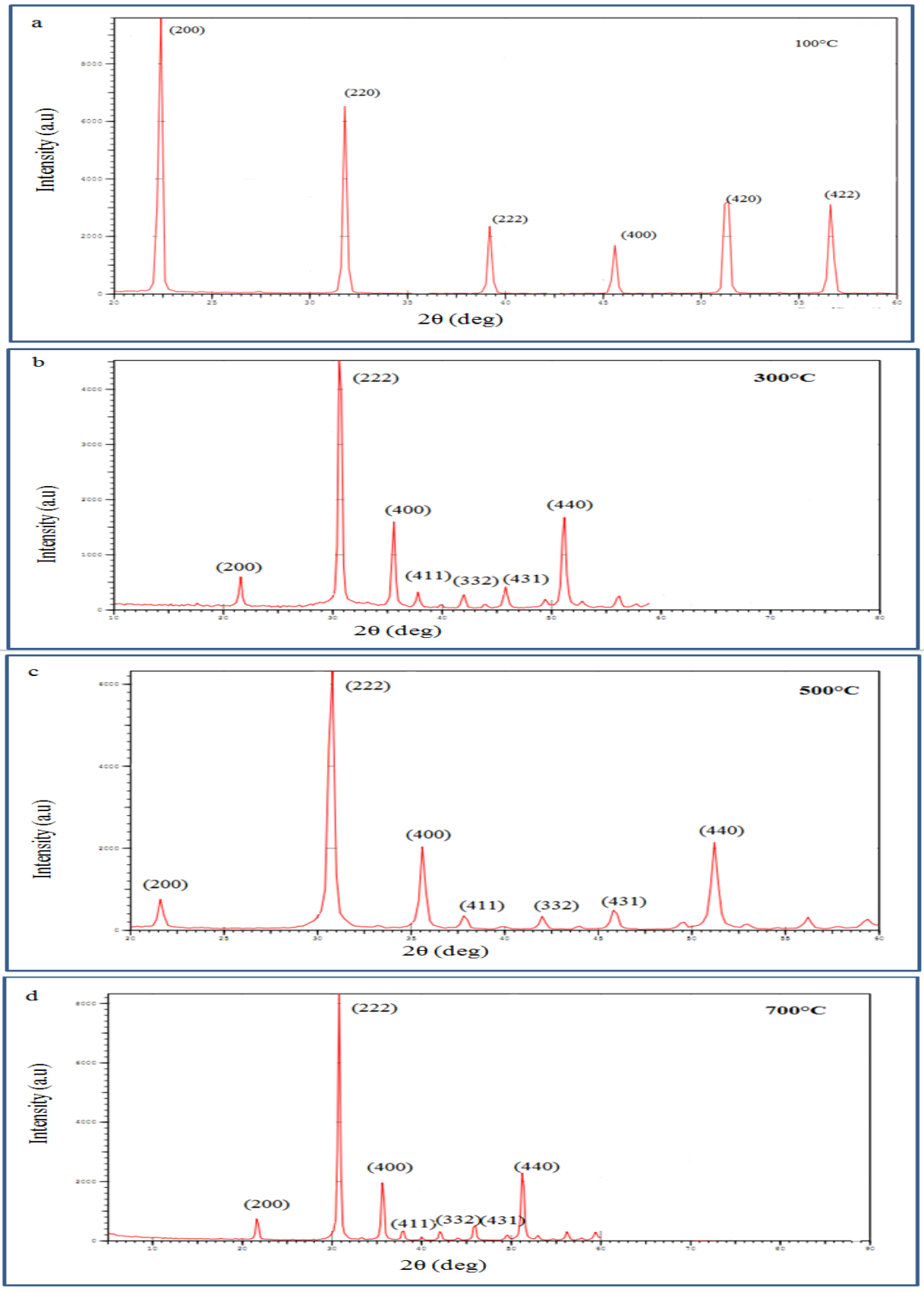


**Figure 2-** XRD patterns of $In(OH)_3$ at annealing temperature (a) 100°C, XRD patterns of $In_2O_3$ at annealing temperature: (b) 300°C, (C) 500°C and (d) 700°C.

Figure- 3(a) shows FTIR spectrum of the indium hydroxide (as-prepared). In this spectrum, a strong absorption bands around 3500 and 1635 $cm^{-1}$ characteristized of OH stretching and bending absorbed water respectively, because of the difficulty of removing the water residue completely [12]. The annealed sample at 300°C, Figure-3(b), three main strong peaks centered at 601, 565 and 418 $cm^{-1}$ were observed, that are characteristic of the In-O and In-O-In stretching respectively, when the annealing temperatures increase to 500 and 700 C, Figures-3(c and d), four main strong peaks around 601, 565, 540 and 426 $cm^{-1}$ were observed, those are characteristic of the In-O, In-In and In-O-In stretching respectively [7]. The absorption bands around 3500 and 1635 $cm^{-1}$ become undistinguished because the samples lose the moist ($H_2O$).

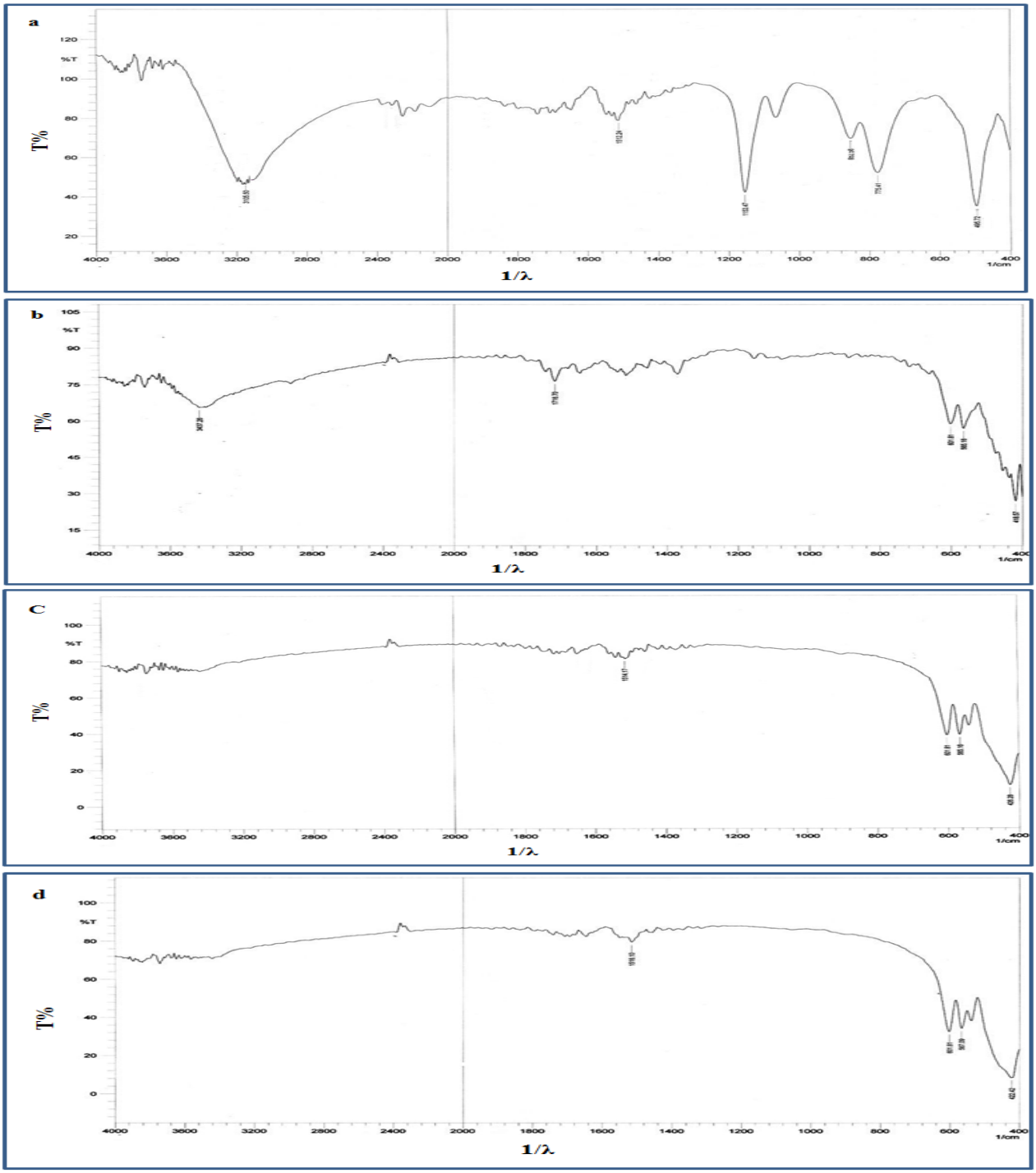


**Figure 3-** FTIR transmittance spectra of $In_2O_3$ at different annealing temperature: (a) 100°C, (b) 300°C, (C) 500°C and (d) 700°C as a function of wavenumber.

Figure-4 shows a typical two and three- dimensional AFM image of $In_2O_3$ nanoparticles with annealing at (a-100, b-300, c-500, and d-700)$^oC$. The average grain size is found to be (78.59-93.81nm). AFM results show that the grain size increases by increasing temperature due to improving the crystallinity of the nanoparticles [3]. Figure -5 shows the granularity cumulation distribution chart of $In_2O_3$ with annealing at (a-100, b-300, c-500, and d-700)$^oC$.

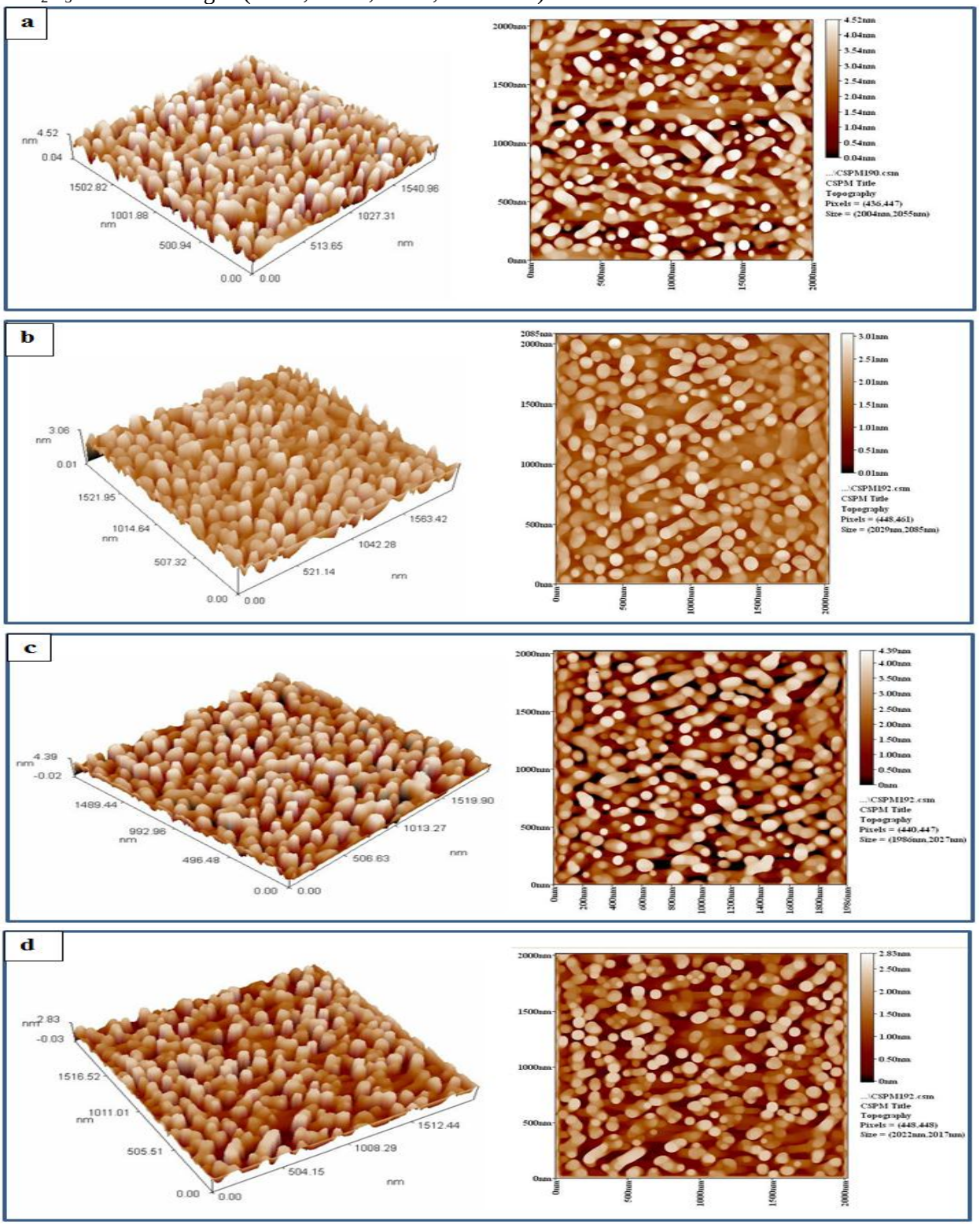


**Figure 4-** (3-D and 2-D AFM images of $In_2O_3$ at different annealing temperatures: (a) 100°C, (b) 300°C, (c) 500°C and (d) 700°C for 90 min.

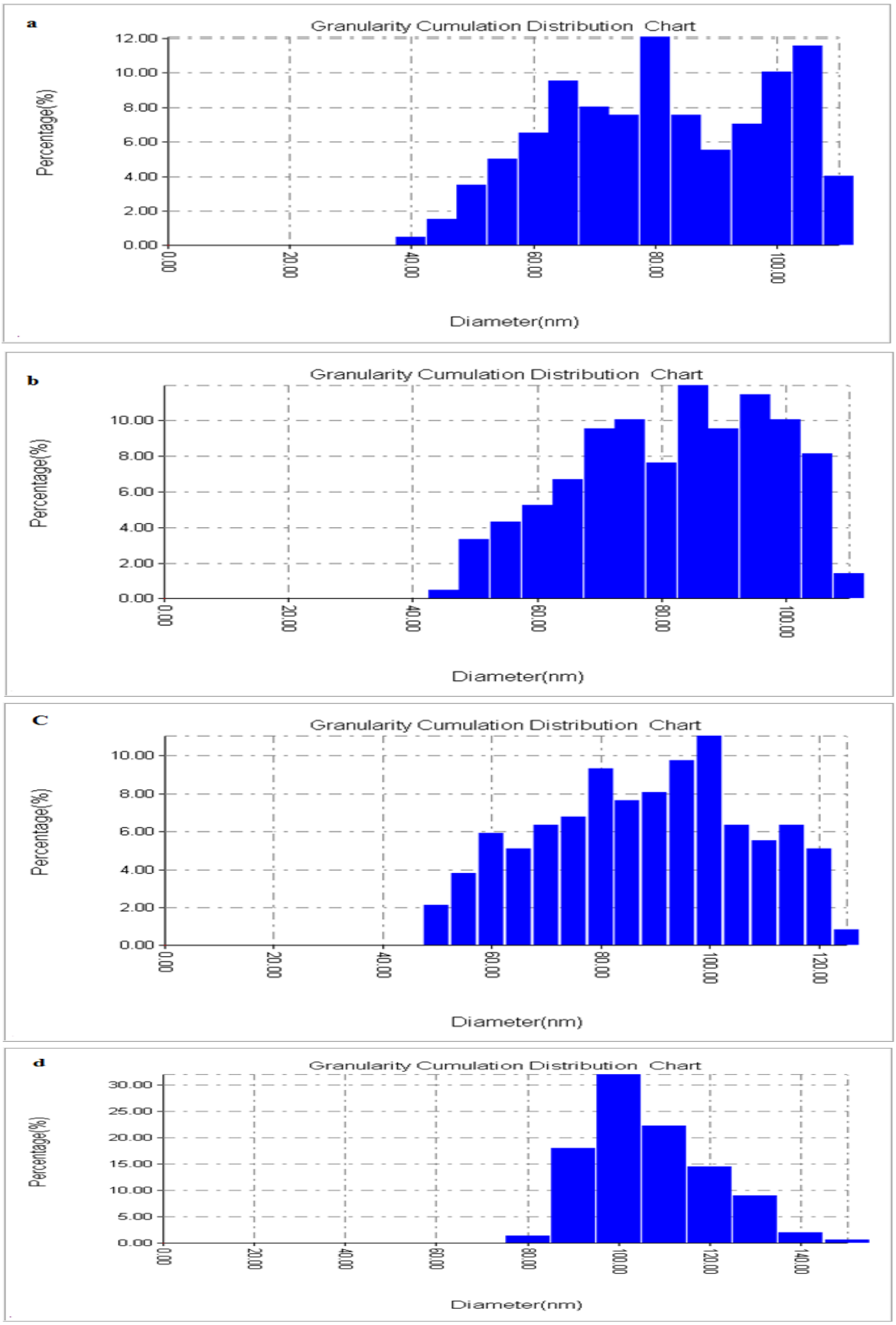


**Figure 5-** Granularity cumulation distribution chart of $In_2O_3$ a: 100°C, b: 300°C c: 500°C and d: 700°C.

Figure-6 shows the SEM images of $In_2O_3$. According to the SEM photographs, the shapes are cubic, increasing temperature effects on the surface morphology, especially grains dimension and improved in structure and the uniformity of the nanoparticle enhanced [3].The grain size is increasing with increasing temperature, which is found to have agglomerated crystallites within each grain and cluster, irregular surface morphology was observed [13].

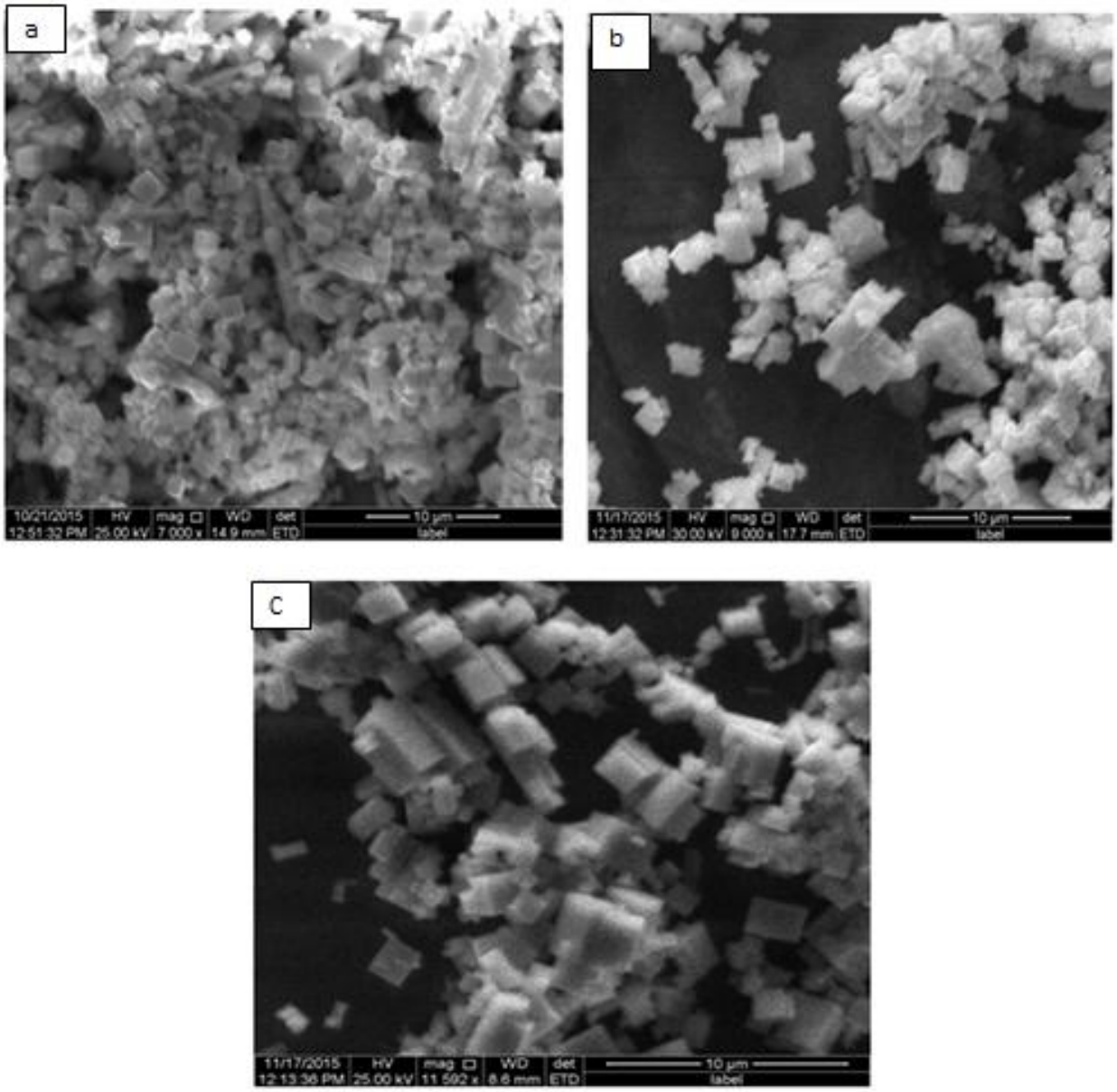


**Figure 6 - SEM images for $In_2O_3$ nanoparticle at a: 100°C, b: 300°C and C: 500°C.**

Figure-7 shows the optical transmittance curves as a function of the wavelength for the $In_2O_3$ nanoparticles at various annealing temperatures (100, 300, 500 and 700)°C for (90 min). It can be observed that the optical transmittance increases with increasing annealing temperature. The optical transmittance changed from (20% to 89%) with the increase of annealing temperature [3]. The highest transmittance value is about (89%) in the UV-Visible region for the $In_2O_3$ nanoparticles at 500˚C. The increase in transmittance is attributed to high crystallinity, structural homogeneity and improvement in the lattice constant. In the case of higher annealing temperatures above 500˚C, there is a drop in transmittance due to the increased irregularity and impaired crystallinity and leads to films with less stoichiometry [13].

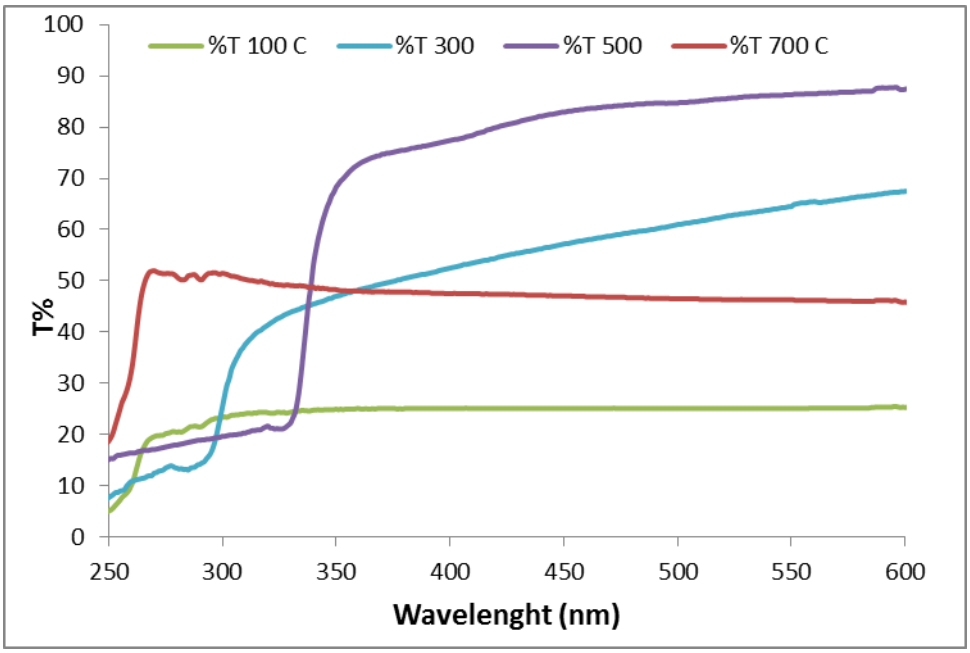


**Figure 7-** The optical transmittance spectra for indium oxide ($In_2O_3$) at different annealing temperatures (100, 300, 500 and 700 ˚C).

Figure-8 shows the optical band gap of the $In_2O_3$ nanoparticle. The optical band gap of $In_2O_3$ nanoparticle is increases with increasing annealing temperature at (300,500 and 700)°C, this is due to improvement of crystallinity and decreasing in the oxygen deficiency [14]. The high value of band gap confirms the surface smoothness and uniformity of $In(OH)_3$ annealed at 100°C. Annealed $In_2O_3$ nanoparticles at 500˚C have a band gap of 3.65 eV [13].

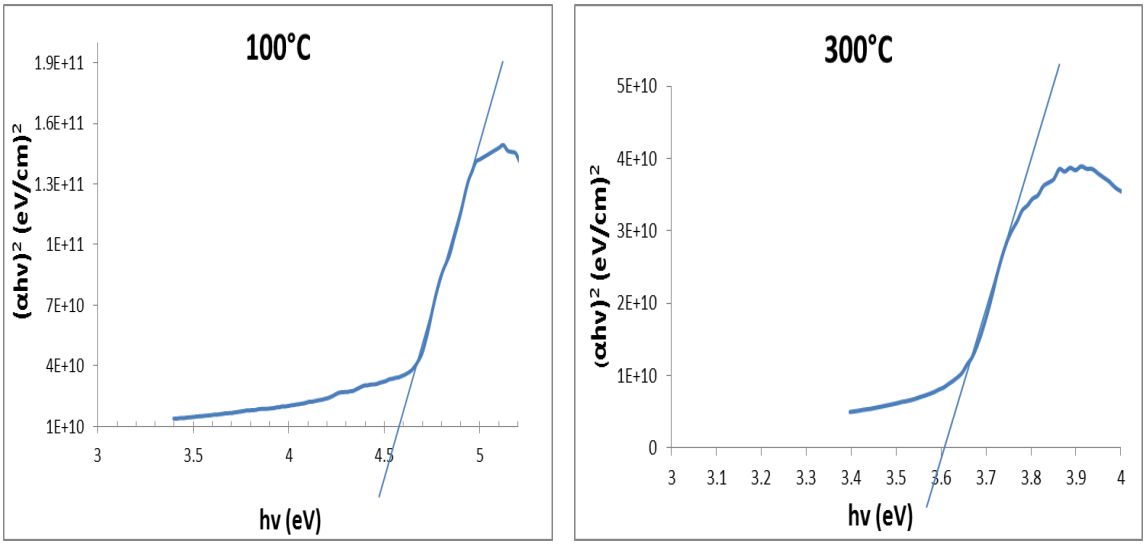

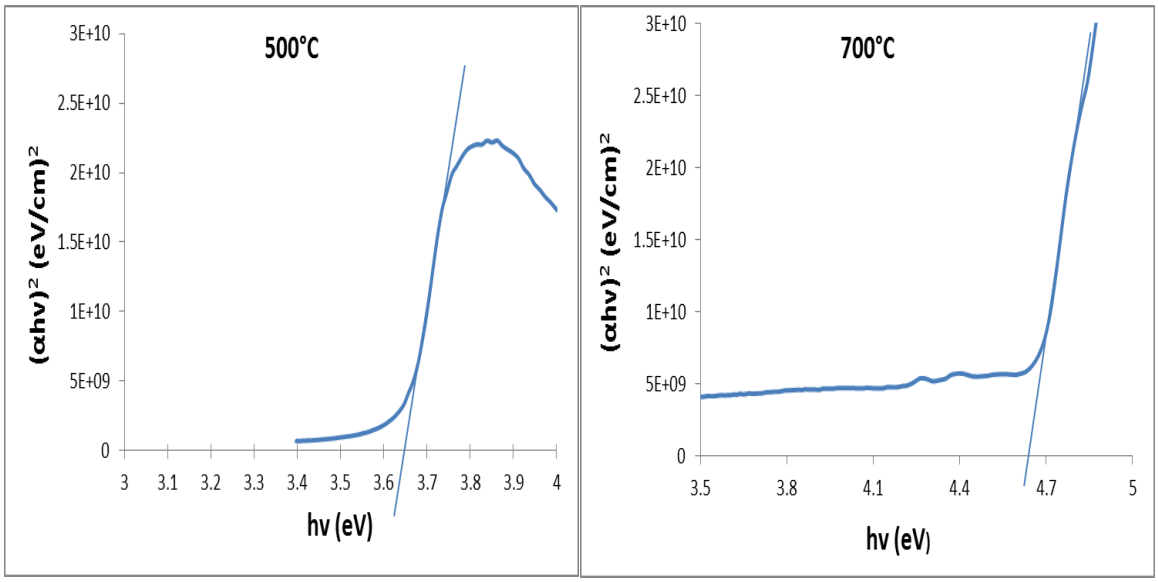


**Figure 7-** The optical band gap for indium oxide ($In_2O_3$) at different annealing temperature (100, 300, 400 and 700 °C).

## 4. Conclusions

In conclusion, we have presented experimental study of the growth of (CdO) thin films using oblique angle deposition. Structural, morphological, optical, thermoelectrically and electrical properties are found to be dependent on the oblique deposition angle farth This study was focused on the Indium oxide that annealing temperature (300, 400 and 700°C), and the size of $In_2O_3$ nanoparticles obtained by Solvothermal technique starting with indium chloride and urea in autoclave device. The annealing $In_2O_3$ nanoparticles were characterized by XRD, AFM, SEM, UV/Visible and FTIR spectroscopy measurements. XRD and SEM found that the $In_2O_3$ have cubic crystallites crystal structure with high intensity of plane (222). We notice that the size of nanoparticles is in direct relationship with the increase of the temperature annealing from 78.59 to 94.4 nm.

## Reference


1. Raid A. Ismail, Abdulrahman K. Ali, Khaleel I. Hassoon, **2013**. Preparation of a silicon heterojunction photodetector from colloidal indium oxide nanoparticles. *Optics & Laser Technology*, 51, pp: 1-4.
2. Chin-Chiuan Kuo, Chi-Chang Liu, Yaug-Fea Jeng, Chung-Chih Lin,Yeuh-Yeong Liou, and Ju-Liang He. **2010.** Thickness Dependence of Optoelectrical Properties of Mo-Doped $In_2O_3$ Films Deposited on Polyethersulfone Substrates by Ion-Beam-Assisted Evaporation. Hindawi Publishing Corporation, *Journal of Nanomaterials*, 8 pages, 840316,
3. Bagheri Khatibani A., Rozati S.M. and Bargbidi Z. **2012.** Preparation, Study and Nanoscale Growth of Indium Oxide Thin Films. *Acta Physica Polonica A*, 122(1), pp: 220-223.
4. Raad S. Sabry, Ibrahim R. Agool, Asaad M. Abbas. **2014**. Calcination Temperature Dependent of Hydrothermal Indium Oxide Nanostructures. *Australian Journal of Basic and Applied Sciences*, 8(16), pp: 165-168,
5. Ajayb Al-Resheedi, Norah Saad Alhokbany, Refaat Mohammed Mahfouz. **2014.** Radiation Induced Synthesis of $In_2O_3$ Nanoparticles - Part 1: Synthesis of $In_2O_3$ Nanoparticles by Sol-gel Method Using Un-irradiated and γ-Irradiated Indium Acetate. *Materials Research*, 17(2), pp: 346-351.
6. Bagheri-Mohagheghi M.-M., Shahtahmasebi N., Mozafari E., Shokooh-Saremi M. **2009.** Effect of the synthesis route on the structural properties and shape of the indium oxide ($In_2O_3$) nano-particles. *Physica* E 41, pp: 1757–1762.
7. Ayeshamariam A., Bououdina M. and Sanjeeviraja C. **2011.** Optical, electrical and sensing properties of $In_2O_3$ nanoparticles. *Materials Science in Semiconductor Processing*, 16, pp: 686–695.

**8.** Kazuhiro Kato, Hideo Omoto, Takao Tomioka, Atsushi Takamatsu .**2011**. Changes in electrical and structural properties of indium oxide thin films through post-deposition annealing. *Thin Solid Films*, 520(1), pp: 110–116.

**9.** Alexander Gurlo a., Maria Ivanovskaya , Nicolae Barsan ,Udo Weimar. **2003**. Corundum-type indium (III) oxide: formation under ambient conditions in $Fe_2O_3$–$In_2O_3$ system. *Inorganic Chemistry Communications*, 6, pp: 569–572.

**10.** Rahnamaye Aliabad H. A., Bazrafshan M., Vaezi H., Masood Yousaf, Junaid Munir, Saeed M. A. **2013**. Optoelectronic Properties of Pure and Co Doped Indium Oxide by Hubbard and modified Becke–Johnson Exchange Potentials. *Chinese Physical Society*, 30 (12), 127101.

**11.** Liu Li, Shouchun Li, Guo Xin, Yue He and Wang Lianyuan **2016**. Excellent performance of gas sensor based on $In_2O_3$–$Fe_2O_3$ nanotubes. *Journal of Semiconductors*, 37 (1), pp: 1674-4926.

**12.** Guodong Liu. **2011.** Synthesis, Characterization of $In_2O_3$ Nanocrystals and Their Photoluminescence Property. *Int. J. Electrochem. Sci*.,6, pp: 2162 – 2170.

**13.** Marikkannu S., Kashif M., Ayeshamariam A., Sethupathi N., Vidhya V. S., Piraman S., Jayachandran M. **2014.** Studies on jet nebuliser pyrolysed indium oxide thin films. *Journal of Ovonic Research*, 10 (4), pp: 115 – 125.

**14.** Mohamed H. A. **2012**. Effect of substrate temperature on physical properties of $In_2O_3$: Sn films deposited by e-beam technique. *Int. J. of Physical Sciences*, 7(13), pp: 2102 – 2109.